



MIT Open Access Articles

Measurements of Indirect CP Asymmetries in D^0 K^+K^- and D^0 K^+K^0 Decays

The MIT Faculty has made this article openly available. **Please share** how this access benefits you. Your story matters.

Citation	Aaij, R., B. Adeva, M. Adinolfi, C. Adrover, A. Affolder, Z. Ajaltouni, J. Albrecht, et al. "Measurements of Indirect CP Asymmetries in D^0 K^+K^- and D^0 K^+K^0 Decays." Physical Review Letters 112, no. 4 (January 2014). © 2014 CERN, for the LHCb Collaboration
As Published	http://dx.doi.org/10.1103/PhysRevLett.112.041801
Publisher	American Physical Society
Version	Final published version
Accessed	Sun Apr 24 20:26:50 EDT 2016
Citable Link	http://hdl.handle.net/1721.1/87744
Terms of Use	Article is made available in accordance with the publisher's policy and may be subject to US copyright law. Please refer to the publisher's site for terms of use.
Detailed Terms	

Measurements of Indirect CP Asymmetries in $D^0 \rightarrow K^-K^+$ and $D^0 \rightarrow \pi^-\pi^+$ Decays

R. Aaij *et al.**

(LHCb Collaboration)

(Received 29 October 2013; published 31 January 2014)

A study of indirect CP violation in D^0 mesons through the determination of the parameter A_Γ is presented using a data sample of pp collisions, corresponding to an integrated luminosity of 1.0 fb^{-1} , collected with the LHCb detector and recorded at the center-of-mass energy of 7 TeV at the LHC. The parameter A_Γ is the asymmetry of the effective lifetimes measured in decays of D^0 and \bar{D}^0 mesons to the CP eigenstates K^-K^+ and $\pi^-\pi^+$. Fits to the data sample yield $A_\Gamma(KK) = (-0.35 \pm 0.62 \pm 0.12) \times 10^{-3}$ and $A_\Gamma(\pi\pi) = (0.33 \pm 1.06 \pm 0.14) \times 10^{-3}$, where the first uncertainties are statistical and the second systematic. The results represent the world's best measurements of these quantities. They show no difference in A_Γ between the two final states and no indication of CP violation.

DOI: 10.1103/PhysRevLett.112.041801

PACS numbers: 13.25.Ft, 11.30.Er, 12.15.Ff, 14.40.Lb

The asymmetry under simultaneous charge and parity transformation (CP violation) has driven the understanding of electroweak interactions since its discovery in the kaon system [1]. CP violation was subsequently discovered in the B^0 and B_s^0 systems [2–4]. Charmed mesons form the only neutral meson-antimeson system in which CP violation has yet to be observed unambiguously. This system is the only one in which mesons of up-type quarks participate in matter-antimatter transitions, a loop-level process in the standard model (SM). This charm mixing process has recently been observed for the first time unambiguously in single measurements [5–7]. The theoretical calculation of charm mixing and CP violation is challenging for the charm quark [8–12]. Significant enhancement of mixing or CP violation would be an indication of physics beyond the SM.

The mass eigenstates of the neutral charm meson system, $|D_{1,2}\rangle$, with masses $m_{1,2}$ and decay widths $\Gamma_{1,2}$, can be expressed as linear combinations of the flavor eigenstates, $|D^0\rangle$ and $|\bar{D}^0\rangle$, as $|D_{1,2}\rangle = p|D^0\rangle \pm q|\bar{D}^0\rangle$ with complex coefficients satisfying $|p|^2 + |q|^2 = 1$. This allows the definition of the mixing parameters $x \equiv 2(m_2 - m_1)/(\Gamma_1 + \Gamma_2)$ and $y \equiv (\Gamma_2 - \Gamma_1)/(\Gamma_1 + \Gamma_2)$.

Nonconservation of CP symmetry enters as a deviation from unity of λ_f , defined as

$$\lambda_f \equiv \frac{q\bar{A}_f}{pA_f} = -\eta_{CP} \left| \frac{q}{p} \right| \left| \frac{\bar{A}_f}{A_f} \right| e^{i\phi}, \quad (1)$$

where A_f (\bar{A}_f) is the amplitude for a D^0 (\bar{D}^0) meson decaying into a CP eigenstate f with eigenvalue η_{CP} , and ϕ

is the CP -violating relative phase between q/p and \bar{A}_f/A_f . Direct CP violation occurs when the asymmetry $A_d \equiv (|A_f|^2 - |\bar{A}_f|^2)/(|A_f|^2 + |\bar{A}_f|^2)$ is different from zero. Indirect CP violation comprises nonzero CP asymmetry in mixing, $A_m \equiv (|q/p|^2 - |p/q|^2)/(|q/p|^2 + |p/q|^2)$ and CP violation through a nonzero phase ϕ . The phase convention of ϕ is chosen such that, in the limit of no CP violation, $CP|D^0\rangle = -|\bar{D}^0\rangle$. In this convention CP conservation leads to $\phi = 0$ and $|D_1\rangle$ being CP odd.

The asymmetry of the inverse of effective lifetimes in decays of D^0 (\bar{D}^0) mesons into CP -even final states, $\hat{\Gamma}(\hat{\Gamma})$, leads to the observable A_Γ defined as

$$A_\Gamma \equiv \frac{\hat{\Gamma} - \hat{\Gamma}}{\hat{\Gamma} + \hat{\Gamma}} \approx \eta_{CP} \left(\frac{A_m + A_d}{2} y \cos \phi - x \sin \phi \right). \quad (2)$$

This makes A_Γ a measurement of indirect CP violation, as the contributions from direct CP violation are measured to be small [13] compared to the precision on A_Γ available so far [14]. Here, effective lifetimes refer to lifetimes measured using a single-exponential model in a specific decay mode. Currently available measurements of A_Γ [15,16] are in agreement with no CP violation at the per mille level [13].

This Letter reports measurements of A_Γ in the CP -even final states K^-K^+ and $\pi^-\pi^+$ using 1.0 fb^{-1} of pp collisions at 7 TeV center-of-mass energy at the LHC recorded with the LHCb detector in 2011. In the SM, the phase ϕ is final-state independent and thus measurements in the two final states are expected to yield the same results. At the level of precision of the measurements presented here, differences due to direct CP violation are negligible. However, contributions to ϕ from physics beyond the SM may lead to different results. Even small final-state differences in the phase $\Delta\phi$ can lead to measurable effects in the observables of the order of $x\Delta\phi$, for sufficiently small phases ϕ in both final states [17]. In addition, the

* Full author list given at the end of the article.

Published by the American Physical Society under the terms of the Creative Commons Attribution 3.0 License. Further distribution of this work must maintain attribution to the author(s) and the published articles title, journal citation, and DOI.

measurements of A_{Γ} in both final states are important to quantify the contribution of indirect CP violation to the observable ΔA_{CP} , which measures the difference in decay-time integrated CP asymmetry of $D^0 \rightarrow K^-K^+$ to $\pi^-\pi^+$ decays [18,19].

The LHCb detector [20] is a single-arm forward spectrometer covering the pseudorapidity range $2 < \eta < 5$, designed for the study of particles containing b or c quarks. The spectrometer dipole magnet is operated in either one of two polarities, the magnetic field vector points either up or down. The trigger [21] consists of a hardware stage, based on information from the calorimeter and muon systems, followed by a software stage, which performs a full event reconstruction. The software trigger applies two sequential selections. The first selection requires at least one track to have momentum transverse to the beam line p_{T} , greater than 1.7 GeV/ c and an impact parameter χ^2 , χ_{IP}^2 , greater than 16. The χ_{IP}^2 is defined as the difference in χ^2 of a given primary interaction vertex reconstructed with and without the considered track. This χ_{IP}^2 requirement introduces the largest effect on the observed decay-time distribution compared to other selection criteria. In the second selection this track is combined with a second track to form a candidate for a D^0 decay into two hadrons (charge conjugate states are included unless stated otherwise). The second track must have $p_{\text{T}} > 0.8$ GeV/ c and $\chi_{\text{IP}}^2 > 2$. The decay vertex is required to have a flight distance χ^2 per degree of freedom greater than 25 and the D^0 invariant mass, assuming kaons or pions as final state particles, has to lie within 50 MeV/ c^2 (or within 120 MeV/ c^2 for a trigger whose rate is scaled down by a factor of 10) around 1865 MeV/ c^2 . The momentum vector of the two-body system is required to point back to the pp interaction region.

The event selection applies a set of criteria that are closely aligned to those applied at the trigger stage. The final-state particles have to match particle identification criteria to separate kaons from pions [22] according to their mass hypothesis and must not be identified as muons using combined information from the tracking and particle identification systems.

Flavor tagging is performed through the measurement of the charge of the pion in the decay $D^{*+} \rightarrow D^0\pi^+$ (soft pion). Additional criteria are applied to the track quality of the soft pion as well as to the vertex quality of the D^{*+} meson. Using a fit constraining the soft pion to the pp interaction vertex, the invariant mass difference of the D^{*+} and D^0 candidates Δm is required to be less than 152 MeV/ c^2 .

About 10% of the selected events have more than one candidate passing the selections, mostly due to one D^0 candidate being associated with several soft pions. One candidate per event is selected at random to reduce the background from randomly associated soft pions. The D^0 decay-time range is restricted to 0.25 to 10 ps such that

there are sufficient amounts of data in all decay-time regions included in the fit to ensure its stability.

The whole data set is split into four subsets, identified by the magnet polarity, and two separate data-taking periods to account for known differences in the detector alignment and calibration. The smallest subset contains about 20% of the total data sample. Results of the four subsets are combined in a weighted average.

The selected events contain about 3.11×10^6 $D^0 \rightarrow K^-K^+$ and 1.03×10^6 $D^0 \rightarrow \pi^-\pi^+$ signal candidates, where the D^{*+} meson is produced at the pp -interaction vertex, with purities of 93.6% and 91.2%, respectively, as measured in a region of 2 standard deviations of the signal peaks in D^0 mass, $m(hh)$ (with $h = K, \pi$), and Δm .

The effective lifetimes are extracted by eight independent multivariate unbinned maximum likelihood fits to the four subsamples, separated by the D^0 flavor as determined by the charge of the soft pion. The fits are carried out in two stages, a fit to $m(hh)$ and Δm to extract the signal yield and a fit to the decay time and $\ln(\chi_{\text{IP}}^2)$ of the D^0 candidate to extract the effective lifetime. The first stage is used to distinguish the following candidate classes: correctly tagged signal candidates, which peak in both variables; correctly reconstructed D^0 candidates associated with a random soft pion (labeled “rnd. π_s ” in the figures), which peak in $m(hh)$ but follow a threshold function in Δm ; and combinatorial background. The threshold functions are polynomials in $\sqrt{\Delta m - m_{\pi^+}}$. The signal peaks in $m(hh)$ and Δm are described by the sum of three Gaussian functions. For the $\pi^-\pi^+$ final state a power-law tail is added to the $m(hh)$ distribution to describe the radiative tail [23]. The combinatorial background is described by an exponential function in $m(hh)$ and a threshold function in Δm .

Partially reconstructed decays constitute additional background sources. The channels that give significant contributions are the decays $D^0 \rightarrow K^-\pi^+\pi^0$, with the charged pion reconstructed as a kaon and the π^0 meson not reconstructed, and $D_s^+ \rightarrow K^-K^+\pi^+$, with the pion not reconstructed. The former peaks broadly in Δm while the latter follows a threshold function and both are described by an exponential in $m(hh)$. Reflections due to incorrect mass assignment of the tracks are well separated in mass and are suppressed by particle identification and are not taken into account. An example fit projection is shown in Fig. 1.

Charm mesons originating from long-lived b hadrons (secondary candidates) form a large background that cannot be separated in the mass fit. They do not come from the interaction point leading to a biased decay-time measurement. The flight distance of the b hadrons causes the D^0 candidates into which they decay to have large χ_{IP}^2 on average. This is therefore used as a separating variable.

Candidates for signal decays, where the D^{*+} is produced at the pp -interaction vertex, are modeled by an exponential

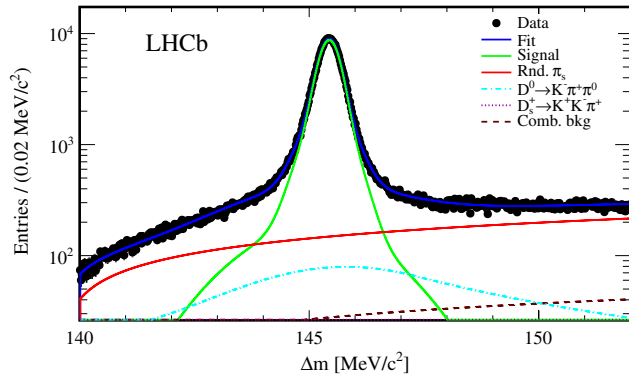


FIG. 1 (color online). Fit of Δm for one of the eight subsets, containing the $D^0 \rightarrow K^- K^+$ candidates with magnet polarity down for the earlier run period.

function in decay time, whose decay constant determines the effective lifetime, and by a modified χ^2 function in $\ln(\chi_{\text{IP}}^2)$ of the form

$$f(x) \equiv \begin{cases} e^{\alpha x - e^{\alpha(x-\mu)}} & x \leq \mu \\ e^{\alpha\mu + \beta(x-\mu) - e^{\beta(x-\mu)}} & x > \mu, \end{cases} \quad (3)$$

where all parameters are allowed to have a linear variation with decay time. The parameters α and β describe the left and right width of the distribution, respectively, and μ is the peak position. Secondary candidates are described by the convolution of two exponential probability density functions in decay time. Since there can be several sources of secondary candidates, the sum of two such convolutions is used with one of the decay constants shared, apart from the smaller $\pi^- \pi^+$ data set where a single convolution is sufficient to describe the data. The $\ln(\chi_{\text{IP}}^2)$ distribution of secondary decays is also given by Eq. (3); however, the three parameters are replaced by functions of decay time

$$\alpha(t) = A + Bt + C \arctan(Dt), \quad (4)$$

and similarly for β and μ , where the parametrizations are motivated by studies on highly enriched samples of secondary decays and where A , B , C , and D describe the decay-time dependence.

The background from correctly reconstructed D^0 mesons associated to a random soft pion share the same $\ln(\chi_{\text{IP}}^2)$ shape as the signal. Other combinatorial backgrounds and partially reconstructed decays for the $K^- K^+$ final state are described by nonparametric distributions. The shapes are obtained by applying an unfolding technique described in Ref. [24] to the result of the $m(hh)$, Δm fit. Gaussian kernel density estimators are applied to create smooth distributions [25].

The detector resolution is accounted for by the convolution of a Gaussian function with the decay-time function. The Gaussian width is 50 fs, an effective value extracted from studies of $B \rightarrow J/\psi X$ decays [26], which has negligible

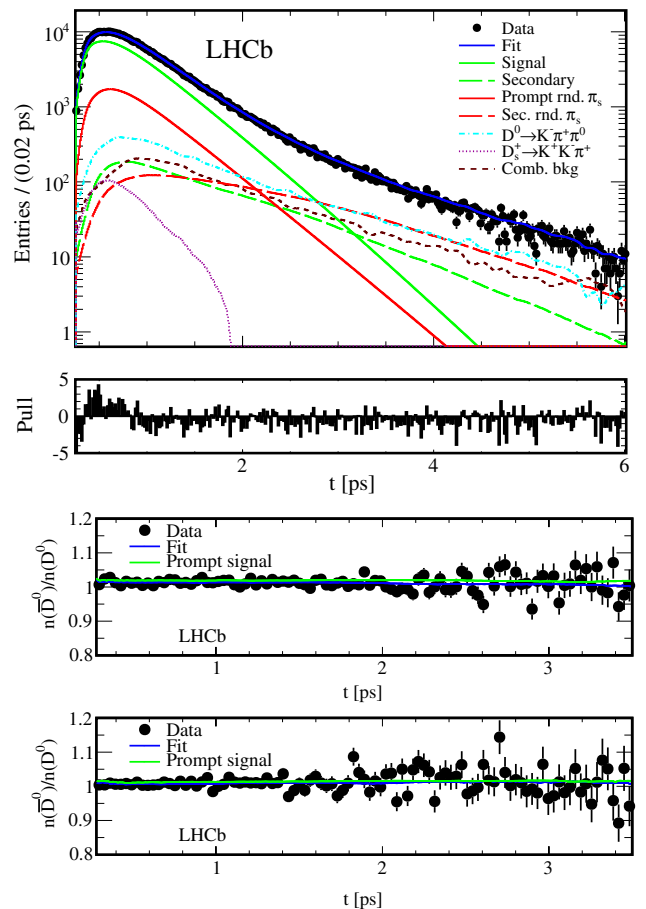


FIG. 2 (color online). Top: fit of decay time to $\bar{D}^0 \rightarrow K^- K^+$ and corresponding pull plot for candidates with magnet polarity down for the earlier run period, where pull is defined as $(\text{data} - \text{model})/\text{uncertainty}$. Middle and bottom: the ratio of \bar{D}^0 to D^0 data and fit model for decays to $K^- K^+$ and $\pi^- \pi^+$ for all data, respectively.

effect on the measurement. Biases introduced by the selection criteria are accounted for through per-candidate acceptance functions which are determined in a data-driven way. The acceptance functions, which take values of 1 for all decay-time intervals in which the candidate would have been accepted and 0 otherwise, enter the fit in the normalization of the decay-time parametrizations. The procedure for determination and application of these functions is described in detail in Refs. [15,27]. Additional geometric detector acceptance effects are also included in the procedure. An example decay-time fit projection is shown in Fig. 2. The fit yields $A_{\Gamma}(KK) = (-0.35 \pm 0.62) \times 10^{-3}$ and $A_{\Gamma}(\pi\pi) = (0.33 \pm 1.06) \times 10^{-3}$, with statistical uncertainties only. The results of the four subsets are found to be in agreement with each other.

The fit has regions where the model fails to describe the data accurately, particularly at small decay times and intermediate values of $\ln(\chi_{\text{IP}}^2)$ as shown in the pull plot in Fig. 2. The same deviations are observed in

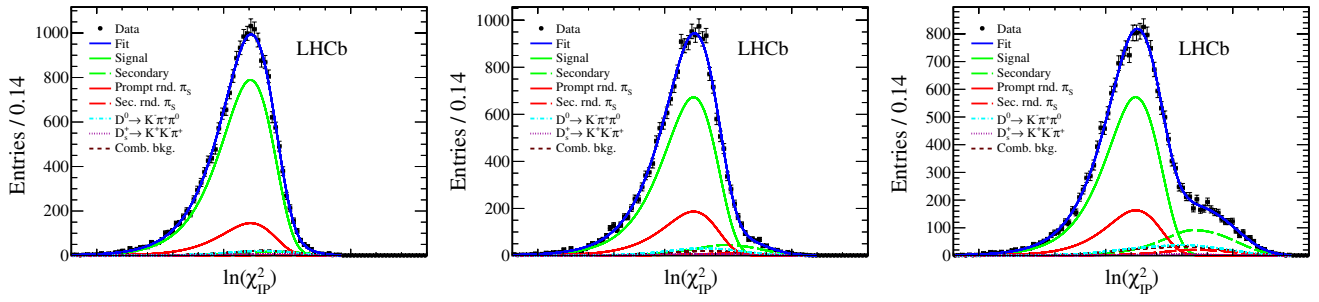


FIG. 3 (color online). Fits of $\ln(\chi_{\text{IP}}^2)$ for $\bar{D}^0 \rightarrow K^- K^+$ candidates for decay-time bins (left to right) 0.25–0.37 ps, 0.74–0.78 ps, and 1.55–1.80 ps.

pseudoexperiment studies, and are reproduced in several independent parametrizations, indicating that the origin is related to the nonparametric treatment of backgrounds in connection with nonideal parametrizations of the $\ln(\chi_{\text{IP}}^2)$ distributions. They do not significantly affect the central value of A_Γ due to the low correlations between the effective lifetime and other fit parameters. The deviations are very similar for fits to D^0 and \bar{D}^0 samples leading to their cancellations in the final asymmetry calculations as shown in Fig. 2.

In addition to the nominal procedure, an alternative method is used, in which the data are binned in equally populated regions of the decay-time distribution and the ratio of \bar{D}^0 to D^0 yields calculated in each bin. This avoids the need to model the decay-time acceptance. The time dependence of this ratio R allows the calculation of A_Γ from a simple linear χ^2 minimization, with

$$R(t) \approx \frac{N_{\bar{D}^0}}{N_{D^0}} \left(1 + \frac{2A_\Gamma}{\tau_{KK}} t \right) \frac{1 - e^{-\Delta t/\tau_{D^0}}}{1 - e^{-\Delta t/\tau_{\bar{D}^0}}}, \quad (5)$$

where $\tau_{KK} = \tau_{K\pi}/(1 + y_{CP})$ is used as an external input based on current world averages [13,28], $N_{\bar{D}^0}/N_{D^0}$ is the signal yield ratio integrated over all decay times and Δt is the bin width. The dependence on τ_{D^0} and $\tau_{\bar{D}^0}$ cancels in the extraction of A_Γ . For this method the signal yields for decays, where the D^{*+} is produced at the pp -interaction vertex, for each decay-time bin are extracted by simultaneous unbinned maximum likelihood fits to $m(hh)$, Δm , and $\ln(\chi_{\text{IP}}^2)$. Each bin is chosen to contain about 4×10^4

candidates, leading to 118 and 40 bins for $K^- K^+$ and $\pi^- \pi^+$, respectively. In general, the binned fit uses similar parametrizations to the unbinned fit, though a few simplifications are required to account for the smaller sample size per bin. The evolution of the fit projections in $\ln(\chi_{\text{IP}}^2)$ with decay time is shown in Fig. 3.

The fits for both methods are verified by randomizing the flavor tags and checking that the results for A_Γ are in agreement with zero. Similarly, the measurement techniques for A_Γ are applied to the Cabibbo-favored $K^- \pi^+$ final state for which they also yield results in agreement with zero. The unbinned fit is further checked by comparing the extracted lifetime using the $K^- \pi^+$ final state to the world average D^0 lifetime, (410.1 ± 1.5) fs [28]. The result of (412.88 ± 0.08) fs, where the uncertainty is only statistical, is found to be in reasonable agreement. If the full difference to the world average were taken as a relative systematic bias it would lead to an absolute bias of less than 10^{-4} on A_Γ . Large numbers of pseudoexperiments, with both zero and nonzero input values for A_Γ , are used to confirm the accuracy of the results and their uncertainties. Finally, dependencies on D^0 kinematics and flight direction, the selection at the hardware trigger stage, and the track and vertex multiplicity, are found to be negligible.

The binned fit yields $A_\Gamma(KK) = (0.50 \pm 0.65) \times 10^{-3}$ and $A_\Gamma(\pi\pi) = (0.85 \pm 1.22) \times 10^{-3}$. Considering the statistical variation between the two methods and the uncorrelated systematic uncertainties, the results from both methods yield consistent results.

The systematic uncertainties assessed are summarized in Table I. The effect of shortcomings in the description

TABLE I. Systematic uncertainties, given as multiples of 10^{-3} . The first column for each final state refers to the unbinned fit method and the second column to the binned fit method.

Source	$A_\Gamma^{\text{unb}}(KK)$	$A_\Gamma^{\text{bin}}(KK)$	$A_\Gamma^{\text{unb}}(\pi\pi)$	$A_\Gamma^{\text{bin}}(\pi\pi)$
Partially reconstructed backgrounds	± 0.02	± 0.09	± 0.00	± 0.00
Charm from b decays	± 0.07	± 0.55	± 0.07	± 0.53
Other backgrounds	± 0.02	± 0.40	± 0.04	± 0.57
Acceptance function	± 0.09	...	± 0.11	...
Magnet polarity	...	± 0.58	...	± 0.82
Total systematic uncertainty	± 0.12	± 0.89	± 0.14	± 1.13

of the partially reconstructed background component in the K^-K^+ final state is estimated by fixing the respective distributions to those obtained in fits to simulated data. The imperfect knowledge of the length scale of the vertex detector as well as decay-time resolution effects are found to be negligible. Potential inaccuracies in the description of the combinatorial background and background from signal candidates originating from b -hadron decays are assessed through pseudoexperiments with varied background levels and varied generated distributions, while leaving the fit model unchanged. The impact of imperfect treatment of background from D^0 candidates associated to random soft pions is evaluated by testing several fit configurations with fewer assumptions on the shape of this background.

The accuracy of the decay-time acceptance correction in the unbinned fit method is assessed by testing the sensitivity to artificial biases applied to the per-event acceptance functions. The overall systematic uncertainties of the two final states for the unbinned method have a correlation of 0.31.

A significant difference between results for the two magnet polarities is observed in the binned method. As this cannot be guaranteed to cancel, a systematic uncertainty is assigned. The unbinned method is not affected by this as it is not sensitive to the overall normalization of the D^0 and \bar{D}^0 samples. In general, the two methods are subject to different sets of systematic effects due to the different ways in which they extract the results. The systematic uncertainties for the binned method are larger due to the fact that the fits are performed independently in each decay-time bin. This can lead to instabilities in the behavior of particular fit components with time, an effect which is minimized in the unbinned fit. The effects of such instabilities are determined by running simulated pseudoexperiments.

The use of the external input for τ_{KK} in the binned fit method does not yield a significant systematic uncertainty. A potential bias in this method due to inaccurate parametrizations of other backgrounds is tested by replacing the probability density functions by different models and a corresponding systematic uncertainty is assigned.

In summary, the CP -violating observable A_Γ is measured using the decays of neutral charm mesons into K^-K^+ and $\pi^-\pi^+$. The results of $A_\Gamma(KK) = (-0.35 \pm 0.62 \pm 0.12) \times 10^{-3}$ and $A_\Gamma(\pi\pi) = (0.33 \pm 1.06 \pm 0.14) \times 10^{-3}$, where the first uncertainties are statistical and the second are systematic, represent the world's best measurements of these quantities. The result for the K^-K^+ final state is obtained based on an independent data set to the previous LHCb measurement [15], with which it agrees well. The results show no significant difference between the two final states and both results are in agreement with zero, thus indicating the absence of indirect CP violation at this level of precision.

We express our gratitude to our colleagues in the CERN accelerator departments for the excellent performance of the LHC. We thank the technical and administrative staff at the LHCb institutes. We acknowledge support from CERN and from the national agencies: CAPES, CNPq, FAPERJ, and FINEP (Brazil); NSFC (China); CNRS/IN2P3 and Region Auvergne (France); BMBF, DFG, HGF, and MPG (Germany); SFI (Ireland); INFN (Italy); FOM and NWO (Netherlands); SCSR (Poland); MEN/IFA (Romania); MinES, Rosatom, RFBR, and NRC "Kurchatov Institute" (Russia); MinECo, XuntaGal, and GENCAT (Spain); SNSF and SER (Switzerland); NAS Ukraine (Ukraine); STFC (United Kingdom); NSF (USA). We also acknowledge the support received from the ERC under FP7. The Tier1 computing centers are supported by IN2P3 (France), KIT, and BMBF (Germany), INFN (Italy), NWO, and SURF (Netherlands), PIC (Spain), and GridPP (United Kingdom). We are thankful for the computing resources put at our disposal by Yandex LLC (Russia), as well as to the communities behind the multiple open source software packages on which we depend.

-
- [1] J. Christenson, J. Cronin, V. Fitch, and R. Turlay, *Phys. Rev. Lett.* **13**, 138 (1964).
 - [2] B. Aubert *et al.* (BABAR Collaboration), *Phys. Rev. Lett.* **87**, 091801 (2001).
 - [3] K. Abe *et al.* (Belle Collaboration), *Phys. Rev. Lett.* **87**, 091802 (2001).
 - [4] R. Aaij *et al.* (LHCb Collaboration), *Phys. Rev. Lett.* **110**, 221601 (2013).
 - [5] R. Aaij *et al.* (LHCb Collaboration), *Phys. Rev. Lett.* **110**, 101802 (2013).
 - [6] T. A. Aaltonen *et al.* (CDF Collaboration), *Phys. Rev. Lett.* **111**, 231802 (2013).
 - [7] R. Aaij *et al.* (LHCb Collaboration), *Phys. Rev. Lett.* **111**, 251801 (2013).
 - [8] M. Bobrowski, A. Lenz, J. Riedl, and J. Rohrwild, *J. High Energy Phys.* **03** (2010) 009.
 - [9] H. Georgi, *Phys. Lett. B* **297**, 353 (1992).
 - [10] T. Ohl, G. Ricciardi, and E. H. Simmons, *Nucl. Phys.* **B403**, 605 (1993).
 - [11] I. I. Bigi and N. G. Uraltsev, *Nucl. Phys.* **B592**, 92 (2000).
 - [12] A. Lenz and T. Rauh, *Phys. Rev. D* **88**, 034004 (2013).
 - [13] Y. Amhis *et al.* (Heavy Flavor Averaging Group) [arXiv:1207.1158](http://arxiv.org/abs/1207.1158); updated results and plots available at <http://www.slac.stanford.edu/xorg/hfag/>.
 - [14] M. Gersabeck, M. Alexander, S. Borghi, V. V. Gligorov, and C. Parkes, *J. Phys. G* **39**, 045005 (2012).
 - [15] R. Aaij *et al.* (LHCb Collaboration), *J. High Energy Phys.* **04** (2012) 129.
 - [16] J. P. Lees *et al.* (BABAR Collaboration), *Phys. Rev. D* **87**, 012004 (2013).
 - [17] A. L. Kagan and M. D. Sokoloff, *Phys. Rev. D* **80**, 076008 (2009).
 - [18] R. Aaij *et al.* (LHCb Collaboration), *Phys. Rev. Lett.* **108**, 111602 (2012).

- [19] R. Aaij *et al.* (LHCb Collaboration), *Phys. Lett. B* **723**, 33 (2013).
- [20] A. A. Alves, Jr. *et al.* (LHCb Collaboration), *JINST* **3**, S08005 (2008).
- [21] R. Aaij *et al.*, *JINST* **8**, P04022 (2013).
- [22] M. Adinolfi *et al.*, *Eur. Phys. J. C* **73**, 2431 (2013).
- [23] T. Skwarnicki, Ph.D. thesis, Institute of Nuclear Physics, Krakow, 1986, DESY-F31-86-02.
- [24] M. Pivk and F. R. Le Diberder, *Nucl. Instrum. Methods Phys. Res., Sect. A* **555**, 356 (2005).
- [25] D. Scott, *Multivariate Density Estimation: Theory, Practice, and Visualization* (John Wiley and Sons, New York, 1992).
- [26] R. Aaij *et al.* (LHCb Collaboration), *Phys. Rev. Lett.* **108**, 101803 (2012).
- [27] V. V. Gligorov, R. Aaij, M. Cattaneo, M. Clemencic, M. Gersabeck, A. Falabella, E. Van Herwijnen, N. Torr, G. Raven, and F. Stagni, *J. Phys. Conf. Ser.* **396**, 022016 (2012).
- [28] J. Beringer *et al.* (Particle Data Group), *Phys. Rev. D* **86**, 010001 (2012), and 2013 partial update for the 2014 edition.

R. Aaij,⁴⁰ B. Adeva,³⁶ M. Adinolfi,⁴⁵ C. Adrover,⁶ A. Affolder,⁵¹ Z. Ajaltouni,⁵ J. Albrecht,⁹ F. Alessio,³⁷ M. Alexander,⁵⁰ S. Ali,⁴⁰ G. Alkhazov,²⁹ P. Alvarez Cartelle,³⁶ A. A. Alves Jr.,²⁴ S. Amato,² S. Amerio,²¹ Y. Amhis,⁷ L. Anderlini,^{17,a} J. Anderson,³⁹ R. Andreassen,⁵⁶ J. E. Andrews,⁵⁷ R. B. Appleby,⁵³ O. Aquines Gutierrez,¹⁰ F. Archilli,¹⁸ A. Artamonov,³⁴ M. Artuso,⁵⁸ E. Aslanides,⁶ G. Auriemma,^{24,b} M. Baalouch,⁵ S. Bachmann,¹¹ J. J. Back,⁴⁷ A. Badalov,³⁵ C. Baesso,⁵⁹ V. Balagura,³⁰ W. Baldini,¹⁶ R. J. Barlow,⁵³ C. Barschel,⁷ S. Barsuk,⁷ W. Barter,⁴⁶ T. Bauer,⁴⁰ A. Bay,³⁸ J. Beddow,⁵⁰ F. Bedeschi,²² I. Bediaga,¹ S. Belogurov,³⁰ K. Belous,³⁴ I. Belyaev,³⁰ E. Ben-Haim,⁸ G. Bencivenni,¹⁸ S. Benson,⁴⁹ J. Benton,⁴⁵ A. Berezhnoy,³¹ R. Bernet,³⁹ M.-O. Bettler,⁴⁶ M. van Beuzekom,⁴⁰ A. Bien,¹¹ S. Bifani,⁴⁴ T. Bird,⁵³ A. Bizzi,^{17,c} P. M. Bjørnstad,⁵³ T. Blake,³⁷ F. Blanc,³⁸ J. Blouw,¹⁰ S. Blusk,⁵⁸ V. Bocci,²⁴ A. Bondar,³³ N. Bondar,²⁹ W. Bonivento,¹⁵ S. Borghi,⁵³ A. Borgia,⁵⁸ T. J. V. Bowcock,⁵¹ E. Bowen,³⁹ C. Bozzi,¹⁶ T. Brambach,⁹ J. van den Brand,⁴¹ J. Bressieux,³⁸ D. Brett,⁵³ M. Britsch,¹⁰ T. Britton,⁵⁸ N. H. Brook,⁴⁵ H. Brown,⁵¹ A. Bursche,³⁹ G. Busetto,^{21,d} J. Buytaert,³⁷ S. Cadet,¹⁵ O. Callot,⁷ M. Calvi,^{20,e} M. Calvo Gomez,^{35,f} A. Camboni,³⁵ P. Campana,^{18,37} D. Campora Perez,³⁷ A. Carbone,^{14,g} G. Carboni,^{23,h} R. Cardinale,^{19,i} A. Cardini,¹⁵ H. Carranza-Mejia,⁴⁹ L. Carson,⁵² K. Carvalho Akiba,² G. Casse,⁵¹ L. Castillo Garcia,³⁷ M. Cattaneo,³⁷ C. Cauet,⁹ R. Cenci,⁵⁷ M. Charles,⁵⁴ P. Charpentier,³⁷ S.-F. Cheung,⁴⁶ N. Chiapolini,³⁹ M. Chrzyszcz,^{39,25} K. Ciba,³⁷ X. Cid Vidal,³⁷ G. Ciezarek,⁵² P. E. L. Clarke,⁴⁹ M. Clemencic,³⁷ H. V. Cliff,⁴⁵ J. Closier,³⁷ C. Coca,²⁸ V. Coco,⁴⁰ J. Cogan,⁶ E. Cogneras,⁵ P. Collins,³⁷ A. Comerma-Montells,³⁵ A. Contu,^{15,37} A. Cook,⁴⁵ M. Coombes,⁴⁵ S. Coquereau,⁸ G. Corti,³⁷ B. Couturier,³⁷ G. A. Cowan,⁴⁹ D. C. Craik,⁴⁷ M. Cruz Torres,⁵⁹ S. Cunliffe,⁵² R. Currie,⁴⁹ C. D'Ambrosio,³⁷ P. David,⁸ P. N. Y. David,⁴⁰ A. Davis,⁵⁶ I. De Bonis,⁴ K. De Bruyn,⁴⁰ S. De Capua,⁵³ M. De Cian,¹¹ J. M. De Miranda,¹ L. De Paula,² W. De Silva,⁵⁶ P. De Simone,¹⁸ D. Decamp,⁴ M. Deckenhoff,⁹ L. Del Buono,⁸ N. Déleage,⁴ D. Derkach,⁵⁴ O. Deschamps,⁵ F. Dettori,⁴¹ A. Di Canto,¹¹ H. Dijkstra,³⁷ M. Dogaru,²⁸ S. Donleavy,⁵¹ F. Dordei,¹¹ A. Dosil Suárez,³⁶ D. Dossett,⁴⁷ A. Dovbnya,⁴² F. Dupertuis,³⁸ P. Durante,³⁷ R. Dzhelezadine,³⁴ A. Dziurda,²⁵ A. Dzyuba,²⁹ S. Easo,⁴⁸ U. Egede,⁵² V. Egorychev,³⁰ S. Eidelman,³³ D. van Eijk,⁴⁰ S. Eisenhardt,⁴⁹ U. Eitschberger,⁹ R. Ekelhof,⁹ L. Eklund,^{50,37} I. El Rifai,⁵ C. Elsasser,³⁹ A. Falabella,^{14,j} C. Färber,¹¹ C. Farinelli,⁴⁰ S. Farry,⁵¹ D. Ferguson,⁹ V. Fernandez Albor,³⁶ F. Ferreira Rodrigues,¹ M. Ferro-Luzzi,³⁷ S. Filippov,³² M. Fiore,^{16,k} C. Fitzpatrick,³⁷ M. Fontana,¹⁰ F. Fontanelli,^{19,i} R. Forty,³⁷ O. Francisco,² M. Frank,³⁷ C. Frei,³⁷ M. Frosini,^{17,37,a} E. Furfaro,^{23,h} A. Gallas Torreira,³⁶ D. Galli,^{14,g} M. Gandelman,² P. Gandini,⁵⁸ Y. Gao,³ J. Garofoli,⁵⁸ P. Garosi,⁵³ J. Garra Tico,⁴⁶ L. Garrido,³⁵ C. Gaspar,³⁷ R. Gauld,⁵⁴ E. Gersabeck,¹¹ M. Gersabeck,⁵³ T. Gershon,⁴⁷ P. Ghez,⁴ V. Gibson,⁴⁶ L. Giubega,²⁸ V. V. Gligorov,³⁷ C. Göbel,⁵⁹ D. Golubkov,³⁰ A. Golutvin,^{52,30} A. Gomes,² P. Gorbounov,^{30,37} H. Gordon,³⁷ M. Grabalosa Gándara,⁵ R. Graciani Diaz,³⁵ L. A. Granado Cardoso,³⁷ E. Graugés,³⁵ G. Graziani,¹⁷ A. Greco,²⁸ E. Greening,⁵⁴ S. Gregson,⁴⁶ P. Griffith,⁴⁴ L. Grillo,¹¹ O. Grünberg,⁶⁰ B. Gui,⁵⁸ E. Gushchin,³² Y. Guz,^{34,37} T. Gys,³⁷ C. Hadjivasiliou,⁵⁸ G. Haefeli,³⁸ C. Haen,³⁷ S. C. Haines,⁴⁶ S. Hall,⁵² B. Hamilton,⁵⁷ T. Hampson,⁴⁵ S. Hansmann-Menzemer,¹¹ N. Harnew,⁵⁴ S. T. Harnew,⁴⁵ J. Harrison,⁵³ T. Hartmann,⁶⁰ J. He,³⁷ T. Head,³⁷ V. Heijne,⁴⁰ K. Hennessy,⁵¹ P. Henrard,⁵ J. A. Hernando Morata,³⁶ E. van Herwijnen,³⁷ M. Heß,⁶⁰ A. Hicheur,¹ E. Hicks,⁵¹ D. Hill,⁵⁴ M. Hoballah,⁵ C. Hombach,⁵³ W. Hulsbergen,⁴⁰ P. Hunt,⁵⁴ T. Huse,⁵¹ N. Hussain,⁵⁴ D. Hutchcroft,⁵¹ D. Hynds,⁵⁰ V. Iakovenko,⁴³ M. Idzik,²⁶ P. Ilten,¹² R. Jacobsson,³⁷ A. Jaeger,¹¹ E. Jans,⁴⁰ P. Jaton,³⁸ A. Jawahery,⁵⁷ F. Jing,³ M. John,⁵⁴ D. Johnson,⁵⁴ C. R. Jones,⁴⁶ C. Joram,³⁷ B. Jost,³⁷ M. Kabbalo,⁹ S. Kandybei,⁴² W. Kanso,⁶ M. Karacson,³⁷ T. M. Karbach,³⁷ I. R. Kenyon,⁴⁴ T. Ketel,⁴¹ B. Khanji,²⁰ O. Kochebina,⁷ I. Komarov,³⁸ R. F. Koopman,⁴¹ P. Koppenburg,⁴⁰ M. Korolev,³¹ A. Kozlinskiy,⁴⁰ L. Kravchuk,³² K. Kreplin,¹¹ M. Kreps,⁴⁷ G. Krocker,¹¹ P. Krokovny,³³ F. Kruse,⁹ M. Kucharczyk,^{20,25,37,e} V. Kudryavtsev,³³ K. Kurek,²⁷ T. Kvaratskheliya,^{30,37} V. N. La Thi,³⁸ D. Lacarrere,³⁷ G. Lafferty,⁵³ A. Lai,¹⁵ D. Lambert,⁴⁹ R. W. Lambert,⁴¹ E. Lanciotti,³⁷ G. Lanfranchi,¹⁸ C. Langenbruch,³⁷ T. Latham,⁴⁷ C. Lazzaroni,⁴⁴ R. Le Gac,⁶ J. van Leerdam,⁴⁰ J.-P. Lees,⁴ R. Lefèvre,⁵ A. Leflat,³¹ J. Lefrançois,⁷ S. Leo,²² O. Leroy,⁶ T. Lesiak,²⁵ B. Leverington,¹¹ Y. Li,³ L. Li Gioi,⁵ M. Liles,⁵¹ R. Lindner,³⁷ C. Linn,¹¹ B. Liu,³ G. Liu,³⁷ S. Lohn,³⁷ I. Longstaff,⁵⁰ J. H. Lopes,² N. Lopez-March,³⁸ H. Lu,³ D. Lucchesi,^{21,d} J. Luisier,³⁸ H. Luo,⁴⁹ O. Lupton,⁵⁴ F. Machefert,⁷ I. V. Machikhiliyan,³⁰ F. Maciuc,²⁸ O. Maev,^{29,37} S. Malde,⁵⁴ G. Manca,^{15,k} G. Mancinelli,⁶

J. Maratas,⁵ U. Marconi,¹⁴ P. Marino,^{22,1} R. Märki,³⁸ J. Marks,¹¹ G. Martellotti,²⁴ A. Martens,⁸ A. Martín Sánchez,⁷ M. Martinelli,⁴⁰ D. Martinez Santos,^{41,37} D. Martins Tostes,² A. Martynov,³¹ A. Massafferri,¹ R. Matev,³⁷ Z. Mathe,³⁷ C. Matteuzzi,²⁰ E. Maurice,⁶ A. Mazurov,^{16,37,j} J. McCarthy,⁴⁴ A. McNab,⁵³ R. McNulty,¹² B. McSkelly,⁵¹ B. Meadows,^{56,54} F. Meier,⁹ M. Meissner,¹¹ M. Merk,⁴⁰ D. A. Milanese,⁸ M.-N. Minard,⁴ J. Molina Rodriguez,⁵⁹ S. Monteil,⁵ D. Moran,⁵³ P. Morawski,²⁵ A. Mordà,⁶ M. J. Morello,^{22,1} R. Mountain,⁵⁸ I. Mous,⁴⁰ F. Muheim,⁴⁹ K. Müller,³⁹ R. Muresan,²⁸ B. Muryn,²⁶ B. Muster,³⁸ P. Naik,⁴⁵ T. Nakada,³⁸ R. Nandakumar,⁴⁸ I. Nasteva,¹ M. Needham,⁴⁹ S. Neubert,³⁷ N. Neufeld,³⁷ A. D. Nguyen,³⁸ T. D. Nguyen,³⁸ C. Nguyen-Mau,^{38,m} M. Nicol,⁷ V. Niess,⁵ R. Niet,⁹ N. Nikitin,³¹ T. Nikodem,¹¹ A. Nomerotski,⁵⁴ A. Novoselov,³⁴ A. Oblakowska-Mucha,²⁶ V. Obraztsov,³⁴ S. Oggero,⁴⁰ S. Ogilvy,⁵⁰ O. Okhrimenko,⁴³ R. Oldeman,^{15,k} M. Orlandea,²⁸ J. M. Otorola Goicochea,² P. Owen,⁵² A. Oyanguren,³⁵ B. K. Pal,⁵⁸ A. Palano,^{13,n} M. Palutan,¹⁸ J. Panman,³⁷ A. Papanestis,⁴⁸ M. Pappagallo,⁵⁰ C. Parkes,⁵³ C. J. Parkinson,⁵² G. Passaleva,¹⁷ G. D. Patel,⁵¹ M. Patel,⁵² G. N. Patrick,⁴⁸ C. Patrignani,^{19,i} C. Pavel-Nicorescu,²⁸ A. Pazos Alvarez,³⁶ A. Pearce,⁵³ A. Pellegrino,⁴⁰ G. Penso,^{24,o} M. Pepe Altarelli,³⁷ S. Perazzini,^{14,g} E. Perez Trigo,³⁶ A. Pérez-Calero Yzquierdo,³⁵ P. Perret,⁵ M. Perrin-Terrin,⁶ L. Pescatore,⁴⁴ E. Pesen,⁶¹ G. Pessina,²⁰ K. Petridis,⁵² A. Petrolini,^{19,i} A. Phan,⁵⁸ E. Picatoste Olloqui,³⁵ B. Pietrzyk,⁴ T. Pilarč,⁴⁷ D. Pinci,²⁴ S. Playfer,⁴⁹ M. Plo Casasus,³⁶ F. Polci,⁸ G. Polok,²⁵ A. Poluektov,^{47,33} E. Polcarpo,² A. Popov,³⁴ D. Popov,¹⁰ B. Popovici,²⁸ C. Potterat,³⁵ A. Powell,⁵⁴ J. Prisciandaro,³⁸ A. Pritchard,⁵¹ C. Prouve,⁷ V. Pugatch,⁴³ A. Puig Navarro,³⁸ G. Punzi,^{22,p} W. Qian,⁴ B. Rachwal,²⁵ J. H. Rademacker,⁴⁵ B. Rakotomiramanana,³⁸ M. S. Rangel,² I. Raniuk,⁴² N. Rauschmayr,³⁷ G. Raven,⁴¹ S. Redford,⁵⁴ S. Reichert,⁵³ M. M. Reid,⁴⁷ A. C. dos Reis,¹ S. Ricciardi,⁴⁸ A. Richards,⁵² K. Rinnert,⁵¹ V. Rives Molina,³⁵ D. A. Roa Romero,⁵ P. Robbe,⁷ D. A. Roberts,⁵⁷ A. B. Rodrigues,¹ E. Rodrigues,⁵³ P. Rodriguez Perez,³⁶ S. Roiser,³⁷ V. Romanovsky,³⁴ A. Romero Vidal,³⁶ M. Rotondo,²¹ J. Rouvinet,³⁸ T. Ruf,³⁷ F. Ruffini,²² H. Ruiz,³⁵ P. Ruiz Valls,³⁵ G. Sabatino,^{24,h} J. J. Saborido Silva,³⁶ N. Sagidova,²⁹ P. Sail,⁵⁰ B. Saitta,^{15,k} V. Salustino Guimaraes,² B. Sanmartin Sedes,³⁶ R. Santacesaria,²⁴ C. Santamarina Rios,³⁶ E. Santovetti,^{23,h} M. Sapunov,⁶ A. Sarti,¹⁸ C. Satriano,^{24,b} A. Satta,²³ M. Savrie,^{16,j} D. Savrina,^{30,31} M. Schiller,⁴¹ H. Schindler,³⁷ M. Schlupp,⁹ M. Schmelling,¹⁰ B. Schmidt,³⁷ O. Schneider,³⁸ A. Schopper,³⁷ M.-H. Schune,⁷ R. Schwemmer,³⁷ B. Sciascia,¹⁸ A. Sciubba,²⁴ M. Seco,³⁶ A. Semennikov,³⁰ K. Senderowska,²⁶ I. Sepp,⁵² N. Serra,³⁹ J. Serrano,⁶ P. Seyfert,¹¹ M. Shapkin,³⁴ I. Shapoval,^{16,42,j} Y. Shcheglov,²⁹ T. Shears,⁵¹ L. Shekhtman,³³ O. Shevchenko,⁴² V. Shevchenko,³⁰ A. Shires,⁹ R. Silva Coutinho,⁴⁷ M. Sirendi,⁴⁶ N. Skidmore,⁴⁵ T. Skwarnicki,⁵⁸ N. A. Smith,⁵¹ E. Smith,^{54,48} E. Smith,⁵² J. Smith,⁴⁶ M. Smith,⁵³ M. D. Sokoloff,⁵⁶ F. J. P. Soler,⁵⁰ F. Soomro,³⁸ D. Souza,⁴⁵ B. Souza De Paula,² B. Spaan,⁹ A. Sparkes,⁴⁹ P. Spradlin,⁵⁰ F. Stagni,³⁷ S. Stahl,¹¹ O. Steinkamp,³⁹ S. Stevenson,⁵⁴ S. Stoica,²⁸ S. Stone,⁵⁸ B. Storaci,³⁹ M. Straticiu,²⁸ U. Straumann,³⁹ V. K. Subbiah,³⁷ L. Sun,⁵⁶ W. Sutcliffe,⁵² S. Swientek,⁹ V. Syropoulos,⁴¹ M. Szczekowski,²⁷ P. Szczypka,^{38,37} D. Szilard,² T. Szumlak,²⁶ S. T'Jampens,⁴ M. Teklishyn,⁷ E. Teodorescu,²⁸ F. Teubert,³⁷ C. Thomas,⁵⁴ E. Thomas,³⁷ J. van Tilburg,¹¹ V. Tisserand,⁴ M. Tobin,³⁸ S. Tolk,⁴¹ D. Tonelli,³⁷ S. Topp-Joergensen,⁵⁴ N. Torr,⁵⁴ E. Tournefier,^{4,52} S. Tourneur,³⁸ M. T. Tran,³⁸ M. Tresch,³⁹ A. Tsaregorodtsev,⁶ P. Tsopelas,⁴⁰ N. Tuning,^{40,37} M. Ubeda Garcia,³⁷ A. Ukleja,²⁷ A. Ustyuzhanin,^{52,q} U. Uwer,¹¹ V. Vagnoni,¹⁴ G. Valenti,¹⁴ A. Vallier,⁷ R. Vazquez Gomez,¹⁸ P. Vazquez Regueiro,³⁶ C. Vázquez Sierra,³⁶ S. Vecchi,¹⁶ J. J. Velthuis,⁴⁵ M. Veltri,^{17,r} G. Veneziano,³⁸ M. Vesterinen,³⁷ B. Viaud,⁷ D. Vieira,² X. Vilasis-Cardona,^{35,f} A. Vollhardt,³⁹ D. Volyanskyy,¹⁰ D. Voong,⁴⁵ A. Vorobyev,²⁹ V. Vorobyev,³³ C. Voß,⁶⁰ H. Voss,¹⁰ R. Waldi,⁶⁰ C. Wallace,⁴⁷ R. Wallace,¹² S. Wandernoth,¹¹ J. Wang,⁵⁸ D. R. Ward,⁴⁶ N. K. Watson,⁴⁴ A. D. Webber,⁵³ D. Websdale,⁵² M. Whitehead,⁴⁷ J. Wicht,³⁷ J. Wiechczynski,²⁵ D. Wiedner,¹¹ L. Wiggers,⁴⁰ G. Wilkinson,⁵⁴ M. P. Williams,^{47,48} M. Williams,⁵⁵ F. F. Wilson,⁴⁸ J. Wimberley,⁵⁷ J. Wishahi,⁹ W. Wislicki,²⁷ M. Witek,²⁵ G. Wormser,⁷ S. A. Wotton,⁴⁶ S. Wright,⁴⁶ S. Wu,³ K. Wyllie,³⁷ Y. Xie,^{49,37} Z. Xing,⁵⁸ Z. Yang,³ X. Yuan,³ O. Yushchenko,³⁴ M. Zangoli,¹⁴ M. Zavertyaev,^{10,s} F. Zhang,³ L. Zhang,⁵⁸ W. C. Zhang,¹² Y. Zhang,³ A. Zhelezov,¹¹ A. Zhokhov,³⁰ L. Zhong,³ and A. Zvyagin^{37,*}

(LHCb Collaboration)

¹Centro Brasileiro de Pesquisas Físicas (CBPF), Rio de Janeiro, Brazil²Universidade Federal do Rio de Janeiro (UFRJ), Rio de Janeiro, Brazil³Center for High Energy Physics, Tsinghua University, Beijing, China⁴LAPP, Université de Savoie, CNRS/IN2P3, Annecy-Le-Vieux, France⁵Clermont Université, Université Blaise Pascal, CNRS/IN2P3, LPC, Clermont-Ferrand, France⁶CPPM, Aix-Marseille Université, CNRS/IN2P3, Marseille, France⁷LAL, Université Paris-Sud, CNRS/IN2P3, Orsay, France⁸LPNHE, Université Pierre et Marie Curie, Université Paris Diderot, CNRS/IN2P3, Paris, France⁹Fakultät Physik, Technische Universität Dortmund, Dortmund, Germany¹⁰Max-Planck-Institut für Kernphysik (MPIK), Heidelberg, Germany¹¹Physikalisches Institut, Ruprecht-Karls-Universität Heidelberg, Heidelberg, Germany¹²School of Physics, University College Dublin, Dublin, Ireland

- ¹³*Sezione INFN di Bari, Bari, Italy*
¹⁴*Sezione INFN di Bologna, Bologna, Italy*
¹⁵*Sezione INFN di Cagliari, Cagliari, Italy*
¹⁶*Sezione INFN di Ferrara, Ferrara, Italy*
¹⁷*Sezione INFN di Firenze, Firenze, Italy*
¹⁸*Laboratori Nazionali dell'INFN di Frascati, Frascati, Italy*
¹⁹*Sezione INFN di Genova, Genova, Italy*
²⁰*Sezione INFN di Milano Bicocca, Milano, Italy*
²¹*Sezione INFN di Padova, Padova, Italy*
²²*Sezione INFN di Pisa, Pisa, Italy*
²³*Sezione INFN di Roma Tor Vergata, Roma, Italy*
²⁴*Sezione INFN di Roma La Sapienza, Roma, Italy*
²⁵*Henryk Niewodniczanski Institute of Nuclear Physics Polish Academy of Sciences, Kraków, Poland*
²⁶*AGH—University of Science and Technology, Faculty of Physics and Applied Computer Science, Kraków, Poland*
²⁷*National Center for Nuclear Research (NCBJ), Warsaw, Poland*
²⁸*Horia Hulubei National Institute of Physics and Nuclear Engineering, Bucharest-Magurele, Romania*
²⁹*Petersburg Nuclear Physics Institute (PNPI), Gatchina, Russia*
³⁰*Institute of Theoretical and Experimental Physics (ITEP), Moscow, Russia*
³¹*Institute of Nuclear Physics, Moscow State University (SINP MSU), Moscow, Russia*
³²*Institute for Nuclear Research of the Russian Academy of Sciences (INR RAN), Moscow, Russia*
³³*Budker Institute of Nuclear Physics (SB RAS) and Novosibirsk State University, Novosibirsk, Russia*
³⁴*Institute for High Energy Physics (IHEP), Protvino, Russia*
³⁵*Universitat de Barcelona, Barcelona, Spain*
³⁶*Universidad de Santiago de Compostela, Santiago de Compostela, Spain*
³⁷*European Organization for Nuclear Research (CERN), Geneva, Switzerland*
³⁸*Ecole Polytechnique Fédérale de Lausanne (EPFL), Lausanne, Switzerland*
³⁹*Physik-Institut, Universität Zürich, Zürich, Switzerland*
⁴⁰*Nikhef National Institute for Subatomic Physics, Amsterdam, Netherlands*
⁴¹*Nikhef National Institute for Subatomic Physics and VU University Amsterdam, Amsterdam, Netherlands*
⁴²*NSC Kharkiv Institute of Physics and Technology (NSC KIPT), Kharkiv, Ukraine*
⁴³*Institute for Nuclear Research of the National Academy of Sciences (KINR), Kyiv, Ukraine*
⁴⁴*University of Birmingham, Birmingham, United Kingdom*
⁴⁵*H.H. Wills Physics Laboratory, University of Bristol, Bristol, United Kingdom*
⁴⁶*Cavendish Laboratory, University of Cambridge, Cambridge, United Kingdom*
⁴⁷*Department of Physics, University of Warwick, Coventry, United Kingdom*
⁴⁸*STFC Rutherford Appleton Laboratory, Didcot, United Kingdom*
⁴⁹*School of Physics and Astronomy, University of Edinburgh, Edinburgh, United Kingdom*
⁵⁰*School of Physics and Astronomy, University of Glasgow, Glasgow, United Kingdom*
⁵¹*Oliver Lodge Laboratory, University of Liverpool, Liverpool, United Kingdom*
⁵²*Imperial College London, London, United Kingdom*
⁵³*School of Physics and Astronomy, University of Manchester, Manchester, United Kingdom*
⁵⁴*Department of Physics, University of Oxford, Oxford, United Kingdom*
⁵⁵*Massachusetts Institute of Technology, Cambridge, Massachusetts, USA*
⁵⁶*University of Cincinnati, Cincinnati, Ohio, USA*
⁵⁷*University of Maryland, College Park, Maryland, USA*
⁵⁸*Syracuse University, Syracuse, New York, USA*
⁵⁹*Pontifícia Universidade Católica do Rio de Janeiro (PUC-Rio), Rio de Janeiro, Brazil (associated with Universidade Federal do Rio de Janeiro (UFRJ), Rio de Janeiro, Brazil)*
⁶⁰*Institut für Physik, Universität Rostock, Rostock, Germany (associated with Physikalisches Institut, Ruprecht-Karls-Universität Heidelberg, Heidelberg, Germany)*
⁶¹*Celal Bayar University, Manisa, Turkey (associated with European Organization for Nuclear Research (CERN), Geneva, Switzerland)*

^a Also at Università di Firenze, Firenze, Italy.

^b Also at Università della Basilicata, Potenza, Italy.

^c Also at Università di Modena e Reggio Emilia, Modena, Italy.

^d Also at Università di Padova, Padova, Italy.

^e Also at Università di Milano Bicocca, Milano, Italy.

^f Also at LIFAELS, La Salle, Universitat Ramon Llull, Barcelona, Spain.

^g Also at Università di Bologna, Bologna, Italy.

^h Also at Università di Roma Tor Vergata, Roma, Italy.

ⁱ Also at Università di Genova, Genova, Italy.

^j Also at Università di Ferrara, Ferrara, Italy.

^k Also at Università di Cagliari, Cagliari, Italy.

^l Also at Scuola Normale Superiore, Pisa, Italy.

^m Also at Hanoi University of Science, Hanoi, Vietnam.

ⁿ Also at Università di Bari, Bari, Italy.

^o Also at Università di Roma La Sapienza, Roma, Italy.

^p Also at Università di Pisa, Pisa, Italy.

^q Also at Institute of Physics and Technology, Moscow, Russia.

^r Also at Università di Urbino, Urbino, Italy.

^s Also at P.N. Lebedev Physical Institute, Russian Academy of Science (LPI RAS), Moscow, Russia